ADDIS ABABA UNIVERSITY
SCHOOL OF GRADUATE STUDIES

FIRST PRINCIPLE DETERMINATION OF ELECTRONIC STRUCTURES OF $BiMnO_3$ USING HUBBARD U CORRECTION

By
Mesfin Atlaw

A thesis submitted for the partial fulfillment of
Masters degree in materials science

Addis Ababa University

June 2009

ADDIS ABABA UNIVERSITY

SCHOOL OF GRADUATE STUDIES

FIRST PRINCIPLE DETERMINATION OF ELECTRONIC STRUCTURES OF $BiMnO_3$ USING HUBBARD U CORRECTION

By

Mesfin Atlaw

MATERIALS SCIENCE PROGRAM

FACULTY OF SCIENCE

Approved by the examining board

Prof. Nicola Marzari	_____
Advisor	
Sib Krishna Ghoshal (Ph.D)	_____
Advisor	
Ahmed Mustefa (Ph.D)	_____
Examiner	
Teketel Yohannes (Ph.D)	_____
Chairman	

Contents **Page**

Acknowledgment

I am greatly indebted to my advisor Prof. Nicola Marzari who patiently guided me through my M.sc thesis for his invaluable contribution to this project. I would like to thank Co-advisor Dr. S.K. Ghoshal for helping me a deeper understanding of the topic under study. I would like to thank Dr. Teketel Yohannes for perfectly organized computational environment and responsive support in all computer related issues. I express my sincere thanks to my families and my friends who assist and support me both mentally and financially in my long journey.

Abstract

In this research work the electronic structure properties and lattice instability of $BiMnO_3$ are examined by employing first principle DFT based techniques. First we perform a pseudopotential calculation using general gradient approximation without Hubbard U. The calculations are further extended adding U term to observe near effects to the Fermi. We also examine phonon dispersion for simple cubic ferromagnetic phase. Results for phonon show clear lattice instability to the off centered displacement driven by strong covalent bonding between Bi (6p) and O (2p) states. The entire work is carried out using Quantum-ESPRESSO. Some of our results are quite new and some matches with other recent findings.

List of figures

List of tables

Acronyms

Bi	Bismuth
BZs	Brillouin Zones
CP/FPMD	Constant Pressure or Finite Pressure Molecular Dynamics
FM	Ferromagnetic
DFT	Density Functional Theory
DOS	Density of state
FT	Fourier Transform
GGA	General Gradient Approximation
GGA+U	General Gradient Approximation plus Hubbard U
HF	Hartree-Fock
LDA	Local Density Approximation
LSD	Local Density Spin
Mn	Manganese
NED	Nudged Elastic Band
NMR	Nuclear Magnetic Resonance
O	Oxygen
PAW	Projected-Augmented Waves
PP	Pseudopotanial
PM	Paramagnetic
PWscf	Plane Wave Self Consistent Field
PUC	Primitive unit cell
TD-DFT	Time Dependent Density Functional Theory
SIC	Self-interaction corrected

Chapter One

Introduction and theoretical background of perovskites

1.1 Introduction

Multiferroic materials, where more than one of ferromagnetic, ferroelectric and ferroelastic properties appear simultaneously, have attracted much attention because of their novel phenomena and possible applications to new devices [1, 2]. Among them, perovskite structure oxides a wide range of low temperature structural distortions associated with lattice instabilities of the prototype cubic structure [3]. The strong coupling between the electric polarization and the structural distortions has led to the wide spread use of the perovskites. From the perovskite-type bismuth transition metal oxides ($BiMO_3$) form a unique material group of particular interest. $BiMnO_3$ is well known to reveal biferroic (ferromagnetic and ferroelectric) properties at low temperature, which can be regarded as the " hydrogen atom " of multiferroics. It is amenable to detailed study using first principle techniques. Investigations of $BiMnO_3$ permit the study of the essential of multiferroism without the problems associated with simulating compounds containing many atoms per formula unit. In addition, $BiMnO_3$ is strikingly different, both magnetically and structurally, from the rare earth perovskite manganites. $BiMnO_3$ is ferromagnetic with a triclinic structural distortion in its ground state [1].

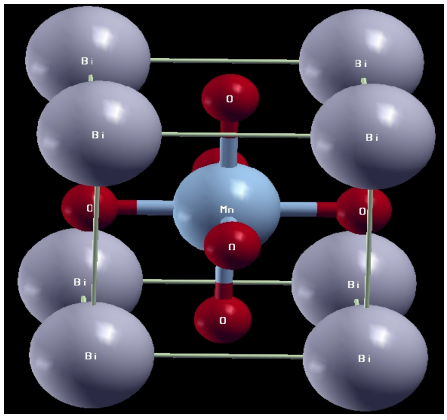

Figure 1.1 The perovskite structure of $BiMnO_3$

Bismuth manganite ($BiMnO_3$) has been regarded as one of the prominent multiferroic

materials. Indeed, the ferromagnetic ordering temperature of ~ 100K and substantial magnetization of ~ 3.2 per formula unit are well established [4, 5]. The largest reported saturation magnetization is 3.92 per formula unit [6].

There are several facts, which support the idea that $BiMnO_3$ is not only ferromagnetic, but also a ferroelectric material

1. The idea of the ferroelectricity has been investigated both experimentally [7,8] and also by the first principles electronic structure calculations, and attributed to the chemical activity of the Bi ($6s^2$) lone pairs, in an analogy with other ferroelectric materials, such as $PbTiO_3$ and $BaTiO_3$. The paramagnetic and ferromagnetic properties of the $BiMnO_3$ are well described by using the experimental lattice parameter 3.95 Å [1].

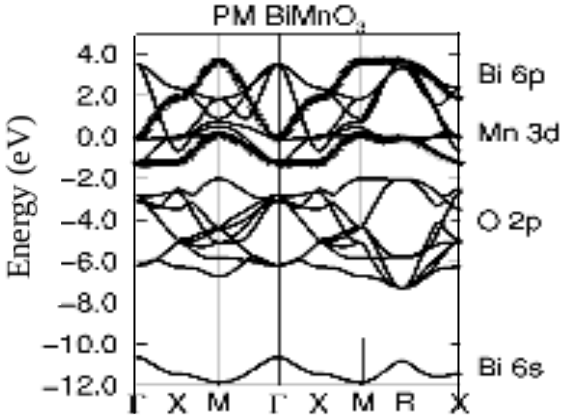

Figure 1.2 Simple cubic paramagnetic band structure of $BiMnO_3$ [1].

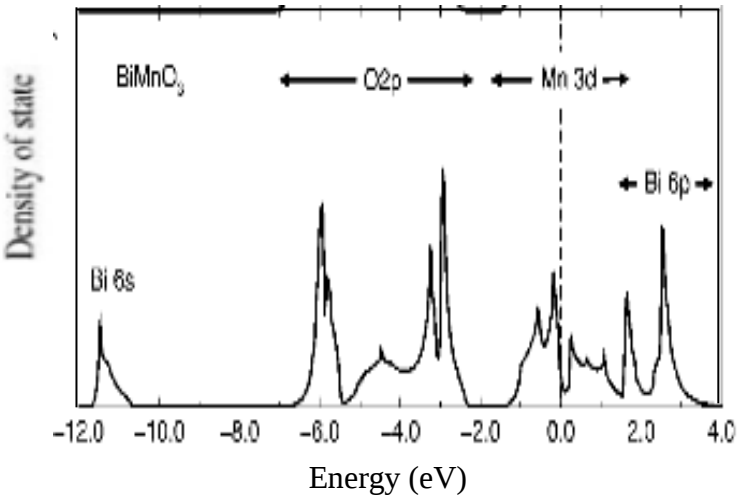

Figure 1.3 Simple cubic paramagnetic density of state of $BiMnO_3$ [1].

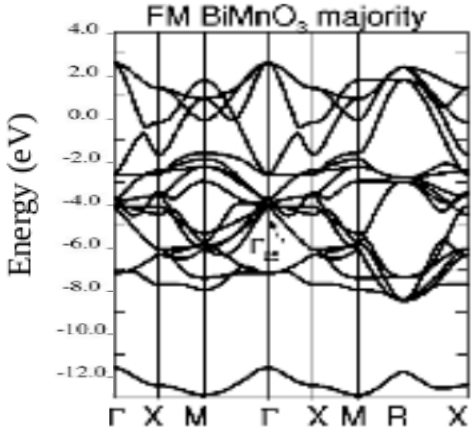

Figure 1.4. Spin up band structure of simple cubic ferromagnetic $BiMnO_3$ [1].

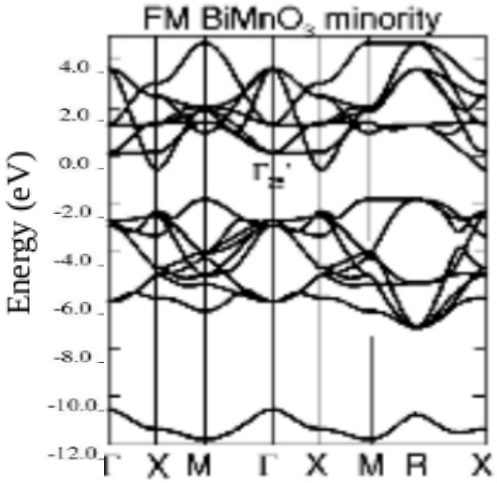

Figure 1.5 Spin down band structure of simple cubic ferromagnetic $BiMnO_3$ [1].

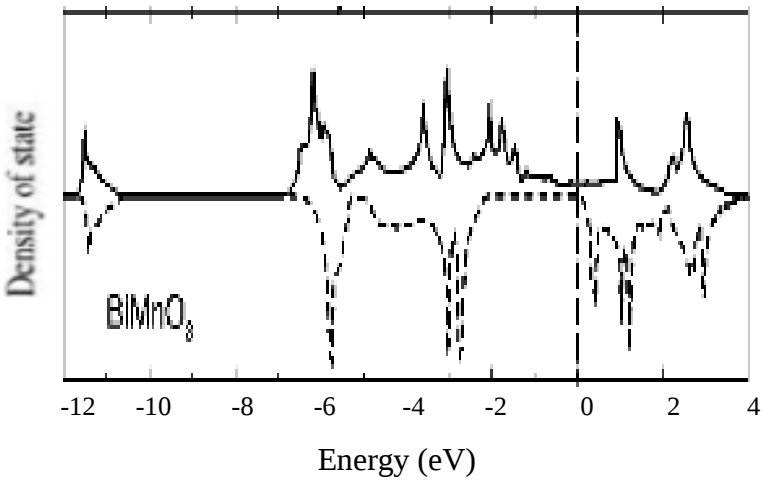

Figure 1.6 Spin up and Spin down density of state of the simple cubic ferromagnetic $BiMnO_3$ [1].

2. Based on the early experimental data from electron and neutron powder diffraction and pair distribution analysis on neutron powder diffraction, $BiMnO_3$ was considered to have non-centrosymmetric C2 space group symmetry in the entire monoclinic region [6,9,10]. However, there is also growing evidence against the intrinsic ferroelectric behavior of $BiMnO_3$

1. Recently the crystal structure of $BiMnO_3$ was re-examined. After careful analysis, they concluded that both monoclinic phases observed in $BiMnO_3$ below 770k have centrosymmetric space group C2/c. If so, $BiMnO_3$ should be anti ferroelectric, rather than ferroelectric material [10].

2. The structure optimization performed by using modern methods of electronic structure calculations revealed that the non centrosymmetric C2 structure, which has been reported earlier, inevitably converges to the new total energy minimum corresponding to the C2/c structure with zero net polarization [10]. According to the modern structure optimization, the ground state of perovskite -structure is centrosymmetric with space group C2/c and zero electric polarization [11].

1.2 Perovskite systems

Perovskite structure oxides exhibit a wide range of low temperature structural distortions associated with lattice instabilities of the prototype cubic structure. The compounds have a general chemical formula ABO_3 where A is monovalent or divalent cation and B is a penta- or tetravalent metal. However, for the purpose of this study, the case where both A and B cations adopt a tetravalent state were considered and the A cations were restricted to being rare earths.

The perfect perovskite structure is very simple and has full cubic symmetry. It can be thought of as a lattice of corner sharing oxygen octahedra with interpenetrating simple cubic lattice of A and B cations. The B cations sit at the center of each oxygen octahedra while the A metal ions lie in 12-fold coordinated sites between the octahedra. The fascinating feature of the perovskite structure is extreme easy with which it will undergo structural phase transition; experimentally the perovskites exhibit a diverse range of phases including transitions to both ferroelectric and antiferroelectric states as well as structural transitions to states involving tilting of the oxygen octahedra [12]. Most of the perovskites are important class of ferroelectric materials [13].

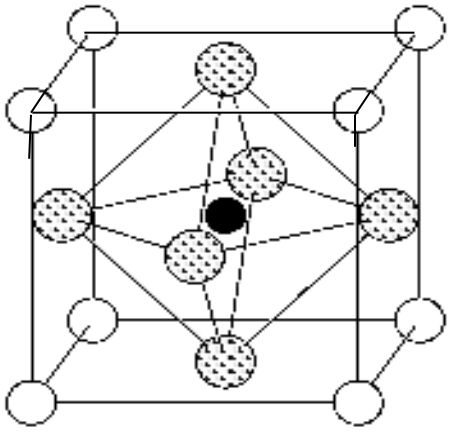

Figure 1.7 The perovskite structure. The small B cation in black is at the center of an octahedron of oxygen anions in gray. The large A cations white occupy the unit cell corners [1].

In magnetic perovskites, different microscopic orientations of the spin-polarized ions give rise to different macroscopic magnetic symmetries. This result in rich in phase diagrams, in which both the magnetic order and the structure depend on the temperature, pressure, and chemical composition. Materials that have strong coupling between all three of the magnetic, electric, and structural order parameters, resulting in simultaneous ferromagnetism, ferroelectricity, and ferroelasticity, are known as multiferroics. Most multiferroic materials are complex structures with many atoms per formula unit, and more than one formula unit per unit cell. The large number of interionic interactions has prevented isolation of the essential factors causing multiferroicity. As a result, the origin of multiferroism and the nature of the coupling between the magnetic, electric polarization, and structural order parameters are not well understood. In spite of the lack of fundamental understanding, a number of device applications have been suggested for multiferroic materials including multiple state memory elements, electric field controlled ferromagnetic resonance devices, and variable transducers with either magnetically modulated piezoeletricity or electrically modulated piezomagnetism. Also, the ability to couple with either the magnetic or the electric polarization offers an extra degree of freedom in the design of conventional actuators, transducers, and storage devices [13,14].

1.3 Thesis Outline

In Chapter One of this thesis we present the general ideal about the perovskites and results in which peoples did both experimentally and computationally in the previous period of time on $BiMnO_3$ and also some related papers that have a close relation ship to the determine the properties of the compound are also presented.

In Chapter Two we will discuss about our technical method, which is Quantum-ESPRESSO and how it generates a data in detail manner with the density functional theory that uses as a backbone for the calculation. We will also see the Success and failures of DFT. At last the correction to the failures to density functional theory are discussed in detail manner with addition of the pseudopotential approximation to the systems. The computational details are discussed so far by taking a specific input to our system in the chapter three. In the chapter four we present our results and discuss it. The results that we will present are emphasis on the cubic structure of $BiMnO_3$ using general gradient approximation without Hubbard U and with a Hubbard U in addition to a phonon dispersion, which shows clear lattice instability of the system under study. In the last chapter of this thesis research conclude so far we did and suggest what it will looks like the material is based on the results we present. The thesis also includes the appendices, which gives more idea to the computational work.

1.4 Objective

General Objective

The general objective of this thesis research is to investigate magnetic, electronic and structural properties of $BiMnO_3$ with a Quantum-ESPRESSO package by employing first principle. Adding a Hubbard U term to the general gradient approximation further extends the calculation to see near effects to the fermi and phonon dispersion to see clear lattice instability of the system under study.

Specific Objective

The specific objective of the research is to determine the

- Band structure
- Density of state and
- Phonon dispersion of the $BiMnO_3$.

and deduce the property of the material in which it can be used for future device designs.

Chapter Two

Electronic structure methods

In the previous chapter we have seen general stoichiometry of perovskite structures especially focusing on $BiMnO_3$ oxide, which reveal different properties at low temperature by referring other findings.

Our goal in this chapter is to discuss Quantum-ESPRESSO that uses density functional theory (DFT), which is a ground state theory emphasis on the charge density as the relevant physical quantity. DFT has proved to be highly successful in describing structural and electronic properties in a vast class of materials, ranging from atoms and molecules to simple crystals to complex extended systems (including glasses and liquids). Furthermore DFT is computationally simple. For these reasons DFT has become a common tool in first principles calculations aimed at describing or even predicting properties of molecular and condensed matter systems.

2.1 The Quantum-ESPRESSO Software

Quantum-ESPRESSO is a distribution of software for atomistic based on electronic structure, using density-functional theory (DFT), a plane waves (PW) basis set and pseudopotentials (PP). Quantum-ESPRESSO stands for Quantum opEn-Source Package for Research in Electronic Structure, Simulation, and Optimization. It is a merge of several pre-existing packages and provides access to several techniques whose usefulness has traditionally been hindered by the lack of available software: notably

– Linear response

– Ultra soft PP

- Car-Parrinello Molecular Dynamics

There are two main packages in Quantum-ESPRESSO

1.CP/FPMD package

2. PWscf package

1.CP/FPMD package

Car-Parrinello variable-cell molecular dynamics with Ultrasoft PP's.

- "Grid Box" for fast treatment of augmentation terms in Ultrasoft PP's
- Various electronic and ionic minimization schemes: damped dynamics, conjugate gradient,
- Verlet dynamics with mass preconditioning
- Constrained dynamics
- Temperature control: Nos´ thermostat for both electrons and ions, velocity rescaling

2. PWscf package

- Self-consistent ground-state energy and Kohn-Sham orbitals, forces, structural optimization
- Spin-orbit and noncolinear magnetization
- Molecular dynamics on the ground-state Born-Oppenheimer surface (no Car-Parrinello dynamics)
- Variable-cell molecular dynamics with modified kinetic functional
- Nudge Elastic Band (NEB) and Fourier Strings Method schemes for transition paths, energy barriers PWscf package, Linear Response
- Phonon frequencies and eigenvectors at a generic wave vector, interatomic force constants in real space, effective charges and dielectric tensors, electron-phonon interaction coefficients for metals
- Third-order anharmonic phonon lifetimes, nonresonant Raman cross sections
- Macroscopic polarization, finite electric fields with Berry's phase

Perspectives and future developments

- Calculation of NMR chemical shifts
- Exact-exchange calculations
- Projector-Augmented Waves (PAW)
- Time-Dependent DFT (TD-DFT) [15].

2.2 Density Functional Theory

The basic concept is that instead of dealing with the many body Schrˆdinger equation, which involves the many body wave function, one deals with a formulation of the problem that involves the total density of electrons n(r). This is a huge simplification, since the many body wave functions need never be explicitly specified as was done in the Hartree and Hartree-Fock approximations. Thus, instead of starting with a drastic approximation for the behavior of the

system (which is what the Hartree and Hartree-Fock wave functions represent), one can develop appropriate single –particle equations in an exact manner, and then introduce approximations as needed.

Thomas-Fermi approximation was the first attempt at using the density as the fundamental variable instead of the wave function. In this approximation the electrons are treat as independent particles and their mutual interaction is described only by Hartree term. The kinetic term is written as the functional of the electronic density. However, it leads to unphysical results for most systems: infinite density at the nucleus of an atom, slow decay of the charge away from the nucleus, absence of chemical bonding and absence of ferromagnetism. This failure is due to over simplified expression for the kinetic energy in terms of the electron density. The use of the density as the fundamental quantity was later formulated rigorously by Hohenberg and Kohn who laid the foundations of the density functional theory (DFT).

In DFT the ground state properties of a system of electrons are all expressed as functional of the ground state electron density. Hohenberg and Kohn formulated two basic theorems of the DFT: For a system of N-interacting electrons with a non-degenerate ground state.

1. The ground state electronic density n(r) uniquely determines the external potential V^{ext}, to within an additional constant.

2 The total energy of the system is minimized by the ground state electron density .The first of the two theorems has the consequence that knowledge of ground state density n(r) completely determines the Hamiltonian of the system .The latter being fixed by the potential which is itself field by the density once the Hamiltonian is known all ground state properties are completely determined. The theorem thus reduces the N-electron problem to determination of a three variable function, i.e, the density n(r). The second theorem allows determining the ground state density through minimization of the energy functional which is known as variational principle.

The total energy of the interacting electronic system in an external potential V^{ext} is written as

$$E[n] = \int V^{ext}(r)n(r)dr + F[N] \tag{2.1}$$

where

$$F[n] = T[n] + V^{ee}[n] \tag{2.2}$$

is a functional of the ground state density alone.

$T[n]$, being kinetic energy,

V^{ee} the electron-electron coulomb repulsion

The functional $F[n]$ is universal and independent of the external potential. Therefore, if a good approximation can be found to $F[n]$ it should be valid for all possible external potentials. Minimizing $E[n]$ with the constraint

$$\int n(r)dr = N, \tag{2.3}$$

N being the total number of electrons gives the ground state total energy and density.

Kohn and Sham suggested the existence of a fictitious system of non-interacting electrons, which has the same ground state density as the original interacting system. For the fictitious system the functional $F[n]$ reads then

$$F[n] = T_O[n] \tag{2.4}$$

and its energy functional is

$$E[n] = \int V^{eff}(r)n(r) + F[n] \tag{2.5}$$

For the original interacting system the functional $F[n]$ is written as a sum of the kinetic energy of the non-interacting system and additional terms due to the electron-electron interactions:

$$F[n] = T_O[n] + \int \frac{n(r)n(r')}{|r-r'|}drdr' + E_{xc}[n] \tag{2.6}$$

This defines an additional, which is known as exchange correlation functional $E_{xc}[n]$, which contains the many-body interactions, not included in the first term. The second term on the right-hand side is the classical Hartree term V^H. The energy functional of the original interacting system can be written as

$$E[n] = F[n] + \int V^{ext}(r)n(r)dr \tag{2.7}$$

$$= T_O[n] + \int n(r)[V^{ext}(r) + V^H(r)dr + E_{xc}[n], \tag{2.8}$$

Minimizing the total energy with respect to the density, as stated in the second theorem gives

$$\frac{\delta E[n]}{\delta n(r)} = \frac{\delta T_O[n]}{\delta n(r)} + V^{ext}(r) + V^H(r) + \frac{\delta E_{xc}[n]}{\delta n(r)} = \mu, \tag{2.9}$$

Where μ is the Lagrange multiplier, which ensures that the number of electrons is N. Application of the variational principle to the non -interacting system yields

$$\frac{\delta E[n]}{\delta n(r)} = \frac{\delta T_O[n]}{\delta n(r)} + V^{eff}(r) = \mu \tag{2.10}$$

Comparing the last two equations, we see that the two systems are identical if we have

$$V^{eff}(r) = V^{ext}(r) + V^{H}(r) + V_{xc}(r) \tag{2.11}$$

where the exchange-correlation potential V_{xc} is defined as

$$V_{xc}(r) = \frac{\delta E_{xc}[n]}{\delta n(r)}, \tag{2.12}$$

It then follows that by solving the single-particle Kohn-Sham (KS) equations

$$H_{KS}\psi_i(r) = [-\Delta_i + V_i^{eff}(r)]\psi_i(r) = \varepsilon_i\psi_i(r), \tag{2.13}$$

of the fictitious system one can determine the single particle density of the interacting system:

$$n(r) = \sum_{i=1}^{occ.} |\psi_i(r)|^2 \tag{2.14}$$

This is a significant simplification of the many –electron problem.

In the Kohn-sham formalism, the ground state total energy, $E[n]$, of the electronic system is given by

$$E = \sum_{i}^{occ.} \varepsilon_i - \iint \frac{n(r)n(r')}{|r-r'|} dr dr' - \int n(r)V_{xc}(r)dr + E_{xc}[n], \tag{2.15}$$

Where the last three terms are corrections for double counting in the sum of the eigenvalues. By treating the kinetic and the electrostatic energies exactly, the exchange correlation part is only a small contribution and its approximate treatment later on should be a minor problem. While this is the case in many systems, so called correlated systems where it is no longer possible to ignore the errors made in approximate exchange correlation [16,17,18].

2.3 Successes and failures of DFT

DFT, even in the simplest LDA approximation, turns out to be much more successful than expected. LDA is computationally much simpler than HF (with the true exchange potential) and no more complex than Slater's local exchange approximation. Yet, LDA yields results that compare well to HF results, even in atoms and molecules – for highly inhomogeneous systems for which an approximation based on the homogeneous electron gas would hardly look appropriate. The best results are however obtained in solids, whose structural and vibrational properties are in

general well described: the correct crystal structure is usually found to the lowest energy; bulk moduli, phonon frequencies are accurate within a few percent.

One may wonder why LDA is so successful, given its resemblance with the not to praised Slater approximation to HF. One reason is somewhat fortuitous: LDA contains a fair amount of error compensation between the exchange and correlation parts. LDA grants a good description of the spherical term of the so-called exchange correlation hole [19].

2.3.1 Accuracy of LDA and gradient correlated functionals

The accuracy of LDA is often considered satisfactory in condensed matter systems, but it is much less so in atomic and molecular physics, for which highly accurate experimental data are available. Also, LDA badly overestimates (~20% and more) cohesive energies and bond strengths in molecules and solids, and as consequence bond lengths are often underestimated.

Such problems are mostly corrected by the introduction of the gradient corrections. The exchange-correlation functional is written as a function of the local density and of the local gradient of the density, as an " enhancement factor " F_{xc} multiplying the homogeneous electron results:

$$E_{xc}[n(r)] = \int \varepsilon_{xc} n(r) F_{xc}(n(r), |\nabla n(r)|) dr \tag{2.16}$$

The enhancement factor is written in terms of r_s and of a dimensionless reduced density gradient s (r):

$$F_{xc}\left(n(r)|\nabla n(r)|\right) \longrightarrow F_{xc}(r_s, s), s(r) = \frac{|\nabla n(r)|}{2k_F n(r)} \tag{2.17}$$

Gradient-corrected functionals are simplest extension of LDA to inhomogeneous systems one can think of. Their adoption has been quite slow: earlier functionals, based on the so-called " gradient expansion ", were a deception, but a later generation of " generalized gradient approximations ", GGA, performed much better and eventually found wide spread energies than LDA, at a modest additional computational cost. In yield description of the hydrogen bond, thus opening the way to calculations for systems, such as water, in which hydrogen bonds play a crucial role (LDA is unstable for those systems: the Hydrogen bond in LDA way is too strong).

The weak vander Waals forces between closed shell systems, that are responsible for the physisorption, are still beyond the reach of DFT. The vander Waals (or dispersive) have a non-

local character: they are due to the charge fluctuations on one system, inducing a dipole on the other. This phenomena is absent by construction from LDA, as well as from any functional based on the local density and on its local derivatives: these can reproduce only phenomena due to charge overlap. Since however LDA overestimates the attractive potential coming from the overlap of the tails of the charge density, closed shell systems in LDA are actually bound with binding energies and binding distances in apparent agreement with experimental results. This is a fictitious result (and a dependence on the separation distance is wrong) that disappears if better-behaved gradient corrected functionals are used [19].

2.3.2 Self-interaction corrected (SIC) approximation

In the density functional each electron interacts with itself via the coulomb electrostatic energy, and this unphysical interaction would be exactly canceled by from the exchange energy. In the local density spin (LSD) approximation this cancellation is imperfect, but numerically rather good. The incorrect treatment of self-interaction in approximate functionals has led some workers to consider self-interaction corrected (SIC) functionals. Within the LSD approximation the SIC functional takes the form

$$E_{SIC} = E_{LSD}[n_{\uparrow}(\vec{r}), n_{\downarrow}(\vec{r})] - \sum_{i\sigma} \delta_{i\sigma}, \tag{2.18}$$

where E_{LSD} is the LSD energy functional and

$$\delta_{i\sigma} = \frac{e^2}{2} \int d\vec{r} \int d\vec{r'} \frac{n_{i\sigma}(\vec{r}) n_{i\sigma}(\vec{r'})}{|r - r'|} + E_{XC}^{LSD}(n_{i\sigma}, o) \tag{2.19}$$

is the self-interaction correction (SIC) for the orbital i with spin and charge density . The first term in above equation is the self-interaction energy, and the second is the LSD approximation to the exchange energy of a fully spin-polarized system with density. This functional is exact for a one-electron system. It leads to the equation

$$\left[-\frac{\hbar^2}{2m} \nabla^2 + V(\vec{r}) + V_{i\sigma}^{SIC}(\vec{r}) \right] \phi_{i\sigma} = \sum_i \lambda_{ij}^{\sigma} \phi_{j\sigma,} \tag{2.20}$$

where $V(\vec{r})$ is the effective potential entering in LSD calculation and V is additional potential. This potential is orbital dependent and the Lagrange parameters are introduced to insure that the solution (referred to as “local orbital “) is orthogonal. The SIC approximation is not invariant

under a unitary transformation of the orbital, and different basis sets lead to different total energies.

Unfortunately, ionization and transfer energies of atoms are not generally better in the LSD-SIC approximation, at least if non-spherical corrections are neglected. The improved total energies in SIC calculations can, in fact, be traced to a much better treatment of the inner most core electrons, which play a relatively minor role in the most chemical and physical processes of interest [19].

2.4 The LDA + U method

A generalization of the local density approximation (LDA) method for systems with strong Coulomb correlations is described which gives a correct description of the Mott insulators. The LDA+U method takes into account orbital dependence of the Coulomb and exchange interactions, which is absent in the LDA. The electrons are separated into two subsystems [20]: localized d or f electrons for which Coulomb d–d interaction should be taken into account by a term $\frac{1}{2}U\sum_{i\neq j} n_i n_j$ (n_i are d-orbital occupancies) as in a mean-field (Hartree–Fock) approximation, and delocalized s, p electrons which could be described by using an orbital-independent one-electron potential (LDA). Let us consider a d ion as an open system with a fluctuating number of d electrons. If we assume that the Coulomb energy of d–d interactions as a function of total number of d electrons $N = \sum n_i$ given by the LDA is a good approximation (but not the orbital energies (eigenvalues)!), then the correct formula for this energy is $E = UN(N-1)/2$. Let us subtract this expression from the LDA total-energy functional and add a Hubbard-like term (neglecting for a while exchange and non-sphericity).

As a result we have the following functional:

$$E = E_{LDA} - UN(N-1)/2 + \frac{1}{2}U\sum_{i\neq j} n_i n_j \qquad (2.20)$$

The orbital energies ε_i are derivatives of (1) with respect to orbital occupations n_i

$$\varepsilon_i = \partial E/\partial n_i = \varepsilon_{LDA} + U\left(\frac{1}{2} - n_i\right) \qquad (2.21)$$

This simple formula shifts the LDA orbital energy by −U/2 for occupied orbitals ($n_j = 1$) and by +U/2 for unoccupied orbitals ($n_i = 0$). A similar formula is found for the orbital-dependent potential ($Vi(r) = \partial E/\partial n_i(r)$ where a variation is taken not on the total charge density n(r) but on

the charge density of a particular *ith* orbital $n_i(r)$):

$$V_i(r) = V_{LDA}(r) + U\left(\frac{1}{2} - n_i\right) \tag{2.22}$$

The LDA+U orbital-dependent potential (3) gives upper and lower Hubbard bands with the energy separation between them equal to the Coulomb parameter U, thus reproducing qualitatively the correct physics for Mott–Hubbard insulators. To construct a quantitatively sound calculational scheme, one needs to define in a more general way an orbital basis set and to take into account properly the direct and exchange Coulomb interactions inside a partially filled d (or f) atomic shell [21]. A similar approximation is used in a model Hamiltonian approach, which has proved to be successful in applications to strongly correlated systems [22,23].

2.5 Plane-wave basis sets

We assume that our system is a crystal with lattice vectors R and reciprocal lattice vectors G. It is not relevant whether the cell is a real unit cell of a real periodic crystal or if it is a supercell describing a periodic system .The Kohn-Sham wavefunctions are classified by a band index and a Bloch vector k in the Brillouin Zone (BZ).

A plane wave basis set is defined as

$$\langle r|k+G\rangle = 1/\sqrt{V}\, e^{i(k+G).r}, \quad \frac{\hbar^2}{2m}|k+G|^2 \le E_{cut,} \tag{2.23}$$

where V is the crystal volume , E_{cut} is the cutoff on the kinetic energy of plane waves [19].

2.6 Pseudopotential approximation

Although Bloch's theorem states that the electronic wave functions can be expanded using a discrete set of plane waves, a plane wave basis set is usually very poorly suited expanding electronic wave functions because a very large number of plane waves are needed to expand the tightly bound core orbital and to follow the rapid oscillations of the wave functions of the valance electrons in the core region. An extremely large plane wave basis set would be required to perform an all-electron calculation, and a vast amount of computational time would be required to calculate the electronic wave functions .The pseudopotential approximation [24,25,26,27]; allows the electronic wave functions to be expanded using a much smaller number of plane wave basis sets.

It is well known that most physical properties of solids are dependent on the valance electrons to a much greater extent than on the core electrons. The pseudopotential approximation exploits this by removing the core electrons and by replacing them and the strong ionic potential by a weaker pseudopotential that acts on a set of pseudo wave functions rather than the true valance wave functions. The valance wave functions oscillate rapidly in the region occupied by the core electrons due to the strong ionic potential in this region. These oscillations maintain the orthogonality between the core wave functions and the valance wave functions, which is required by the exclusion principle. The pseudopotential is constructed, ideally, so that its scattering properties or phase shifts for the pseudo wave functions are identical to the scattering properties of the ion and the core electrons for the valance wave functions, but in such a way that the pseudo wave functions have no radial nodes in the core region. In the core region, the total phase shift produced by the ion and the core electrons will be greater by Л for each node that the valance functions had in the core region, than the phase shift produced by the ion and the valance electron. Outside the core region the two potentials are identical, and the scattering from the two potential is indistinguishable. The phase shift produced by the ion core is different for each angular momentum component of the valance wave function, and so the scattering from the pseudopotential must be angular momentum dependent. The most general form for the pseudopotential is

$$V_{NI} = \sum_{lm} |\mathrm{Im}\rangle V \langle lm|, \tag{2.24}$$

Acting on the electronic wave function with this operator decomposes the wave function into spherical harmonics, each of which is then multiplied by relevant pseudo potential.

A pseudopotential that uses the same potential for all the angular momentum components of the wave function is called a local pseudopotential. A local pseudopotential is only of a distance from the nucleus. It is possible to produce arbitrary, predetermined phase shifts for each angular momentum state with a local potential, but there are limits to the amount that the phase shifts can be adjusted for the different angular momentum states, while maintaining the crucial smoothness and weakness of the pseudopotential. Without a smooth, weak pseudopotential it becomes difficult to expand the wave functions using a reasonable number of plane wave basis states.

2.6.1. Norm conservation

In total energy calculations, the exchange correlation energy of the electronic system is a

function of the electron density. If the exchange – correlation energy is to be desired accurately, it is necessary that outside the core regions the pseudo wave functions and real wave functions be identical, not just in their spatial dependences but also in their absolute magnitudes, so that the two wave functions generate identical charge densities. Adjustment of the pseudopotential to ensure that the integrals of the squared amplitudes of the real and pseudo wave functions inside the core regions are identical guarantees the quality of the wave function and pseudo wave function outside the core region. One of the first attempts to construct pseudopotentials were introduced a class of pseudopotentials that described the valance energies and wave functions of many heavy atoms accurately [28, 29].

Of course, in general, the scattering from the ion core is best described by a non-local pseudopotential that uses a different potential for each angular momentum component of the wave function. A method for the construction of pseudopotentials that corrects even the higher order energy dependence of the scattering has recently been introduced [30]. Local and non-local pseudopotentials of these types are currently termed abinitio or norm conserving and capable of describing the scattering due to the ion in a variety atomic environment, a property referred to as transferability.

2.6.2. Generation procedure

The typical method for generating an ionic pseudopotential for an atom of species is proceeds as follows. All-electron calculations are performed for an isolated atom in its ground state and some exited states, using a given form for the exchange – correlation density functional. This provides valance electron eigenvalues and valance electron wave functions for the atom. A parameterized form for the ionic pseudopotential is chosen. The parameters are then adjusted, so that the pseudo atom calculation using the same form for exchange correlation as in the all electron atom gives both pseudo wave functions that much the valance wave functions outside some cutoff radius and pseudo eigenvalues. The ionic pseudopotential obtained in this fashion is then used, without further modification, for any environment of the atom. The electronic density in any new environment of the atom is then determined using both the ionic pseudopotential obtained in this way and the same form of exchange correlation functional as employed in the construction of the ionic pseudopotential. A generalization of this pseudopotential is Hamann has recently introduced construction procedure for solutions of the atom that are not normalizable.

Finally, it should be noted that ionic pseudopotentials are constructed with cutoff radius ranging typically from one to two times of the value of the core radius. It should be also noted that, in general, the smaller the value of cutoff radius, the more the transferable the potential.

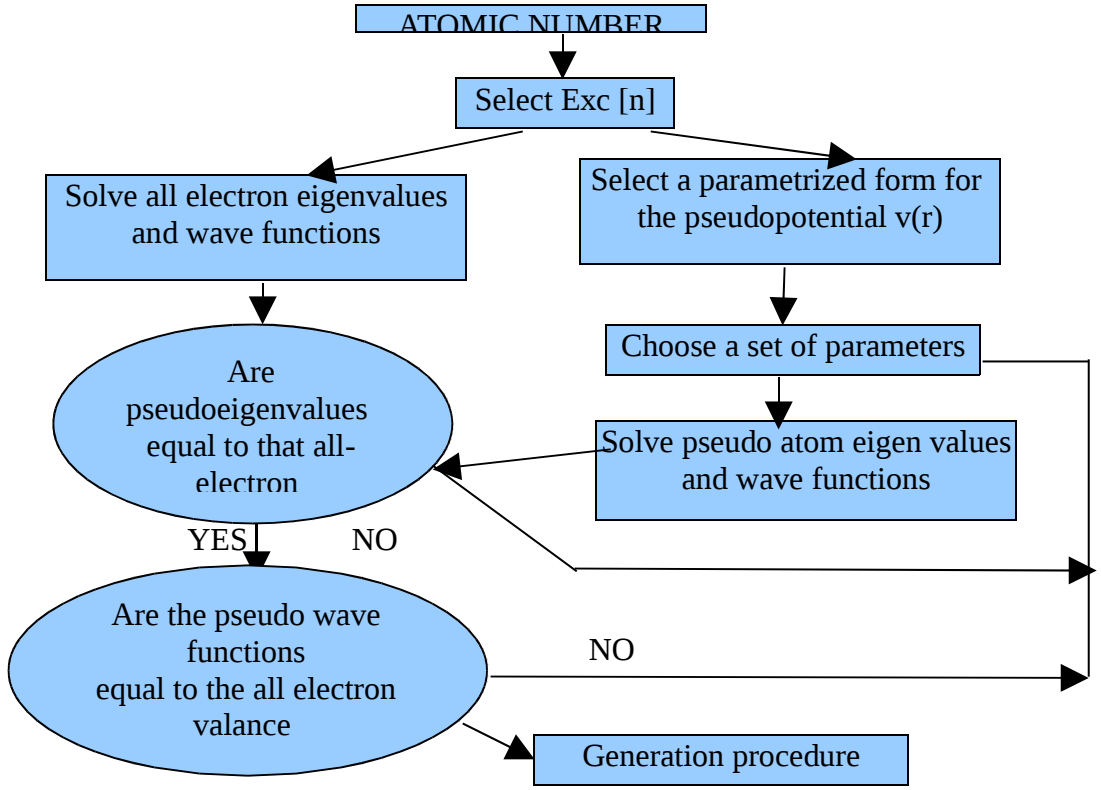

Figure 2.1 flow chart describing the construction of an ionic potential for an atom

2.6.3. Convergence properties

The replacement of the true ionic potential by a weaker pseudopotential allows the electronic wave functions to expanded far fewer plane wave basis states are no longer present. The pseudopotential has a number of other advantages in addition to reducing the number of plane wave basis states needed to expand the electronic wave functions. The removal of the core electrons means that fewer electronic wave functions have to be calculated. More importantly, the total energy of the valance electron system is typically a thousand times smaller than the energy of the all electron system. The difference between the electronic energies of different ionic configurations appears totally in the energy of the valance electrons, so that the accuracy required determining energy differences between ionic configurations in a pseudopotential calculation. The

energy differences are just as large when only the valance electrons are included in the calculation but the total energies are typically a thousand times smaller in the pseudopotential calculation than in the all- electron calculation. But, of course, the total energy is no longer meaningful. Only differences have meaning [31].

2.7 Brillouin-Zone sampling

In order to calculate the charge density n(r) in a periodic system one has to sum over an infinite number of k-points

$$n(r) = \sum_k \sum_i \left|\psi_{k,i}(r)\right|^2 \tag{2.24}$$

where the index i run over occupied bands. Assuming periodic (Born-Von Karman) boundary conditions

$$\psi(r + L_1 R_2) = \psi(r + L_2 R_2) = \psi(r + L_3 R_3) = \psi(r), \tag{2.25}$$

a crystal has $L = L_1 L_2 L_3$ L allowing k-points (L is also the number of unit cells). In the " thermodynamic " limit of an infinite crystal $L \to \infty$, the discrete sum over the k becomes an integral over the Brillouin zone.

Experience shows that this integral can be approximated by a discrete sum over an affordable number of k-points, at in insulators and semiconductors. When present, symmetry can be used to further reduce the number of calculations to be performed. Only the k-point is left to represent each star – the set of k-points that are equivalent by symmetry – with a weight w_i that is proportional the number of k-points in the star. The infinite sum over the Brillouin zone is replaced by a discrete sum over a set of points $\{k_j\}$ and weights w_i

$$\frac{1}{L}\sum_k f_k(r) \to \sum_i w_i f_{ki}(r) \tag{2.26}$$

The resulting sum is then symmetrized to get charge density.

Suitable sets for Brillouin zone sampling in insulators and semiconductors are called " special points ". This name is somewhat misleading: in most cases just form uniform grids in the Brillouin zone.

In metals things are more difficult because one needs an accurate sampling of the Fermi surface. A suitable extension of DFT to factionary occupation numbers is needed. The Gaussian broadening and a tetrahedron techniques, or variations of the above, are generally used.

In super cells, the k-point grid is often limited to the Γ point (k=0). A better sampling may be needed only if it is important to accurately describe the band structure of a subjacent structure crystal structure. This is the case of point defects in solids and of surfaces. If, on the contrary, super cells are used to stimulate completely a periodic or a finite systems, the Γ point is the good choice: a better k-point grid would better account for the periodicity of the system, but this is fictitious anyway [19].

2.8 Phonons

Phonons are one of the most important quasi particles in solids. They have a decisive influence on most electronic and photonic properties of semiconductors. They are most related to losses and often crucially determine the performance of devices [32].

In the classical picture within the harmonic approximation the atoms of a crystal are visualized as joined by harmonic springs and the crystal dynamics is analysed in terms of a linear combination of $3N$ normal modes of vibration. A normal mode of vibration is expressed as a traveling wave of the form $A\exp[i(qr - wt)]$, where q shows the direction of wave propagation, w is the circular frequency of the wave and A is the amplitude of vibration. The energies of the normal modes of a crystal are quantized: for the q^{th} mode the energies are $(nq + 1/2)\hbar w(q)$, $nq = 0,1,2,.....$. The quantum of energy $\hbar w(q)$ is associated with elementary excitation called a phonon. Thus a phonon is a quantum of crystal vibrational energy. The concept of a phonon is similar to that of a photon, which is a quantum of energy in an electromagnetic field. Clearly in the harmonic approximation we have the physical picture of non-interacting phonons in a crystal. As the concept of the phonon originates from relative motions of the atoms, rather than the motion of their center of mass, a phonon in a crystal does not carry a momentum. However, for a practical purpose we assign a momentum $\hbar q$ to a phonon in the q^{th} mode. For this reason a phonon is called a quasi-particle [33, 34].

Chapter Three

Computational Methodology

3.1 Computational details

In our research we use a Quantum-ESPRESSO with in density functional theory. The DFT works by minimizing functions of functions, functionals, to determine the ground state of a molecule. Instead of using functionals based upon individual electron, pseudopotential is used to simplify the calculation. We used an ultrasoft pseudopotential of gradient exchange functionals (PBE). The main package that we use is PWscf, which uses self-consistent electronic structure, structural relaxation, dynamics and linear response calculations (phonons, dielectric properties). The Algorithm of self-consistent iteration is as follows

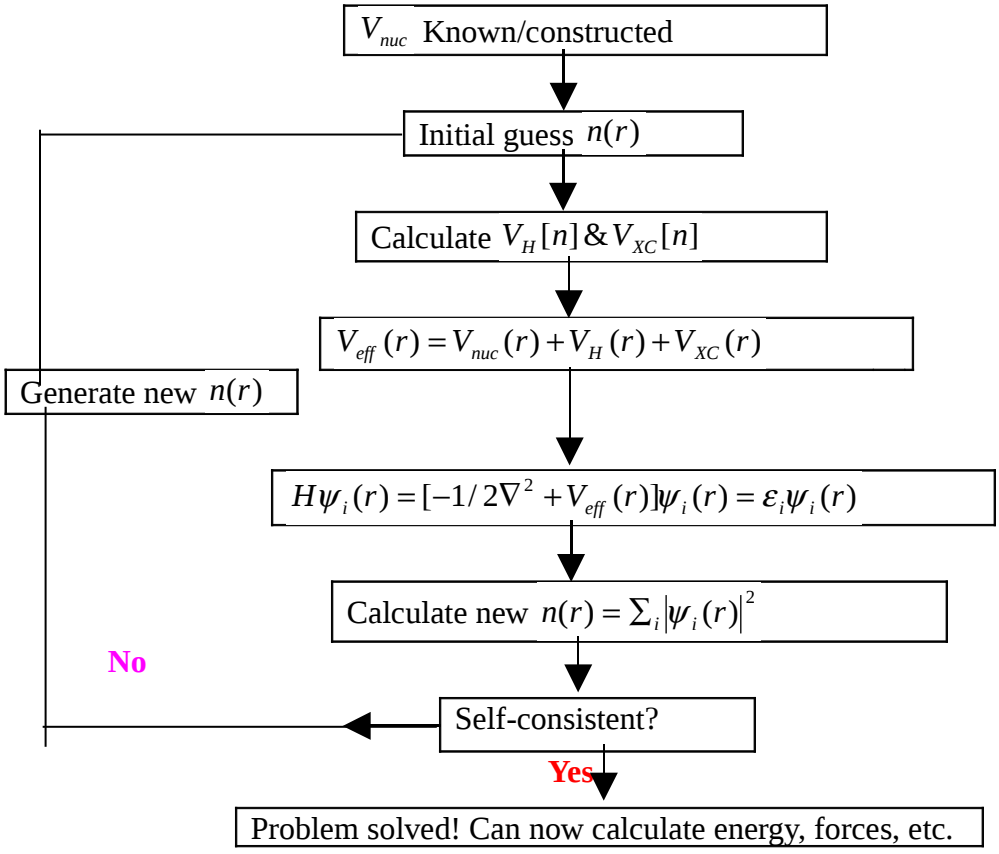

Figure 3.1 The Density Functional Algorithm Scheme

In the above algorithm we consider the charge density as the quantity to be determined self-

consistently. We supply an input charge density to the Kohn-Sham equations and we get an out put charge density. At self-consistency the first algorithm come to mind is simply use the out put charge density as the new input charge density. The new input charge density is generated by mixing the input and output charges. If the new wavefunction (charge density) or the energy is consistent with the old one we reach at the point of self-consistency. After the problem is solved the solved equation can be used to calculate the energy, forces, bulk modules, etc.

3.2 A typical input file for a simple self-consistent calculation

In our calculation the input is composed of several “namelists”, followed by several “cards”. In our research we use the following input

```
 &control
   calculation = 'scf'
   restart_mode = 'from_scratch',
   prefix = 'BMno.scf'
   forc_conv_thr=1.0E-06
   tstress=.true.
   tprnfor=.true.
   pseudo_dir = '/home/student/atlaw',
    outdir='./’
 &system
   brav = 1
   celldm(1) = 7.4,
   nat =  5,
   ntyp = 3,
   ecutwfc = 80,
   ecutrho = 360,
   starting_ magnetization(2) = 0.7
   occupations = 'tetrahedra'
   nspin=1
 &electrons
    diagonalization='david',
```

```
  mixing_beta = 0.5
  conv_thr =1.0E-11
ATOMIC_SPECIES
  Bi    208.98      Bi.pbe-d-mt.UPF
  Mn    54.94       Mn.pbe-sp-van_mit.UPF
  O     15.9994     O.pbe-rrkjus.UPF
ATOMIC_POSITIONS (alat)
  Bi       0.0   0.0   0.0
  Mn       0.5   0.5   0.5
  O        0.5   0.0   0.5
  O        0.0   0.5   0.5
  O        0.5   0.5   0.0
K_POINTS automatic
  6 6 6 1 1 1
```

We see that there are several number of possible options, but we need only to know about the following variables in the namelists:

calculation : 'scf' for self-consistency

'nscf' for band-structure calculation: follows a self-consistent calculation in which the self-consistent charge density was computed

'relax' for structural optimization

ibrav : 1 for simple cubic, 2 for fcc, 3 for bcc, etc

celldm : celldm (1) is the lattice parameter, in atomic units

nat, ntyp: number of atoms and of different atomic types

ecutwfc : kinetic energy cutoff for the plane-wave basis set

nbnd : number of Kohn-Sham states to be calculated

In this research we did for a simple cubic structure of $BiMnO_3$ with a lattice parameter of 3.916 Å. We use a kinetic energy cutoff 80Ry in the unit cell and charge density of 360Ry.We also use a $6\times6\times6$ k-point grid by shifting in $1\times1\times1$ direction to all energy based calculations and $4\times4\times4$ k-point grid for a phonon calculation. The kinetic energy cutoff and charge density were fixed due to an ultra soft pseudopotential specification.

Chapter four

Results and discussion

4.1 Results for simple cubic paramagnetic structure of $BiMnO_3$

In this thesis research we begin by calculating the electronic structure for the high symmetry cubic phases, without including magnetic effects, then lower magnetic symmetry to the ferromagnetic phase. Finally we introduce structural distortions in both paramagnetic and ferromagnetic calculations. This ability to isolate structural and magnetic distortions is unique to computational studies, and allows identifications of the essential microscopic interactions, which cause the observed macroscopic behavior.

First we present results for $BiMnO_3$ in the highest possible symmetry state that is the cubic structure, without spin polarization (we call this the paramagnetic (PM) phase). Although this phase is experimentally inaccessible it provides a useful reference for understanding the ferromagnetic (FM) structures to be discussed later in this paper. The results of the ideal cubic structure of both paramagnetic and ferromagnetic (i.e. Where the atoms are in their original position), which is in agreement with other obtained results [1]. Both the calculations (paramagnetic and ferromagnetic) are calculated by using 3.916 Å.

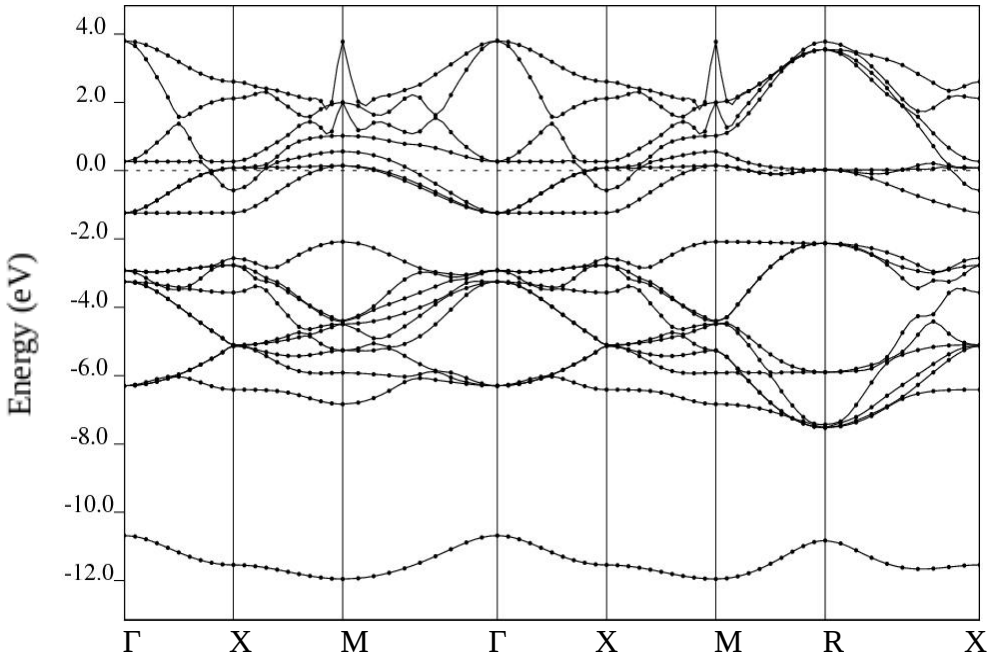

Figure 4.1 Paramagnetic band structure of the ideal cubic structure of $BiMnO_3$.

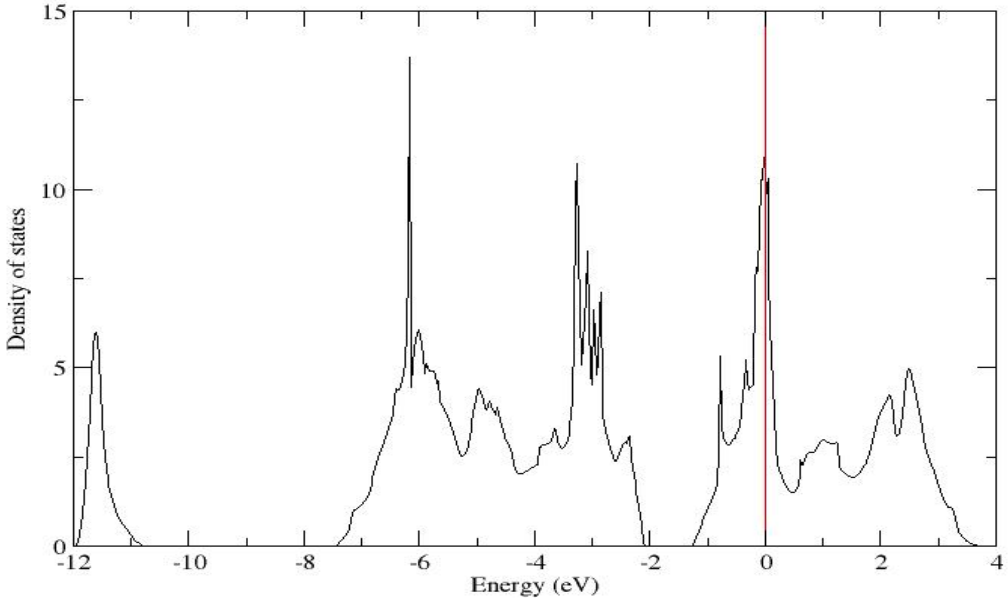

Figure 4.2 Paramagnetic density of state for ideal cubic structure of $BiMnO_3$

The plotted energy range is from -12 eV to 4 eV in which Fermi level is set to zero. In the DOS plots the band between -12 eV and -10 eV is the Bi 6s. The broad series, which lies between -8 eV and -2 eV, is the O 2p. Above to this is the Mn 3d. From the figures we observe that the highest occupied Bi 6s electrons which can be seen clearly in the band structure suggests that it is involved in covalent bonding. It is also seen that the Mn 3d bands overlap with the partially occupied Bi 6p orbitals. In the band structure calculation the Fermi level lies near the top of the Mn 3d t_2g bands. As shown in Figure 4.1 the Mn 3d Sub divided into two bands, lower energy t_2g band and upper energy eg band.

4.2 Results for ideal simple cubic ferromagnetic structure of $BiMnO_3$

As shown in the Figure 4.1 and Figure 4.2 around the Fermi there is high density of states. The large density around the Fermi suggests that the paramagnetic phase is unstable, and that a lower energy structure could be achieved by allowing spin polarization or structural distortion. The results are presented as follows.

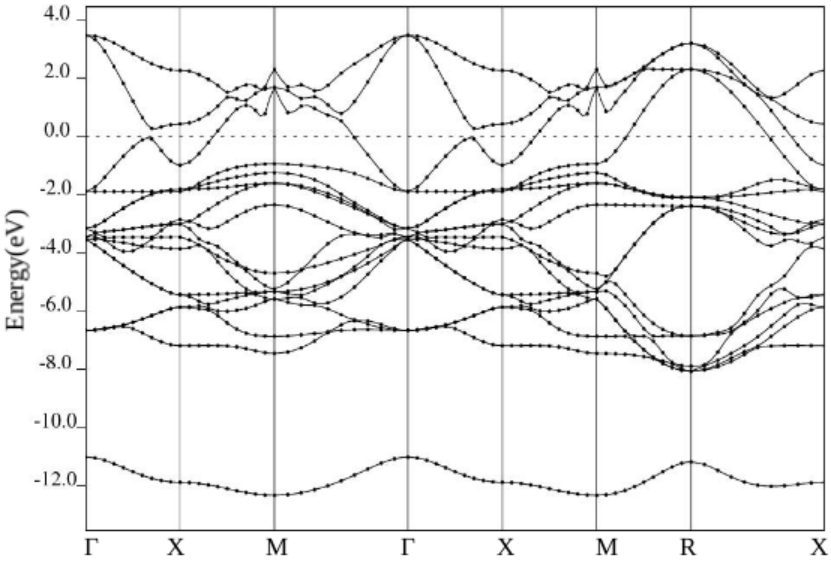

Figure 4.3. Spin up band structure calculation of the ideal cubic ferromagnetic structure of $BiMnO_3$

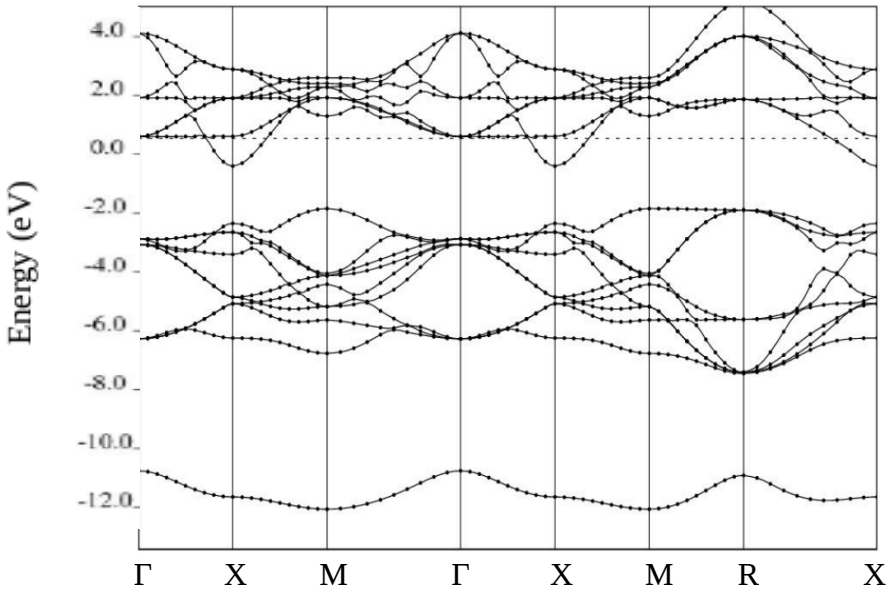

Figure 4.4 Spin down band structure calculation of the ideal cubic ferromagnetic structure of $BiMnO_3$

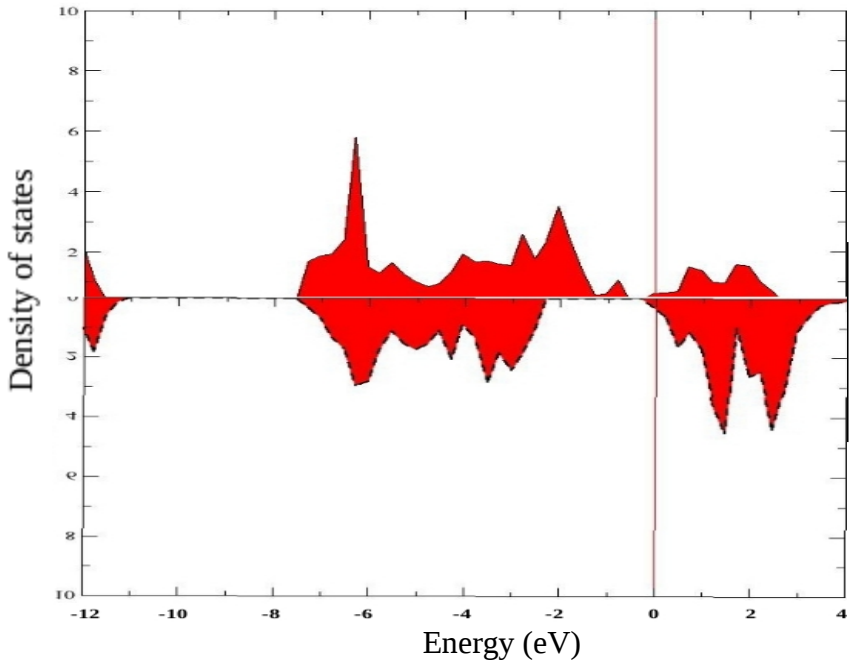

Figure 4.5 Spin up (top) and Spin down (bottom) density of state for the ideal cubic ferromagnetic structure of $BiMnO_3$

Figure 4.5 shows the calculated densities of states for cubic ferromagnetic $BiMnO_3$. The majority spins are represented by solid line on the positive y-axis. In the down spin Mn 3d band is split off from the O 2p band. The up spin Mn 3d hybridizes strongly with the O 2p and there is no band gap for the majority carriers. The DOS at the Fermi level in ferromagnetic $BiMnO_3$ is somewhat lower suggesting that the ferromagnetic phase should be more stable than the paramagnetic phase.

For the ferromagnetic cubic structure of $BiMnO_3$ the Fermi level cuts through the very bottom of the down-spin Mn 3d bands and the conduction band is occupied almost entirely by the up-spin electrons. Materials in which the electrons at the Fermi level are spin polarized are known as half metallics, and are considered desirable for use in devices such as spin transistors. The up-spin Mn 3d strongly hybridizes with the O 2p and there is no band gap for the majority carriers. The up spin DOS at the Fermi level is still high indicating that the cubic ferromagnetic state is still high in energy.

List of parameters	Paramagnetic	Ferromagnetic
Experimental lattice parameter (Å)	3.95 [1]	3.95 [1]
Calculated lattice parameter (Å)	3.915	3.916
Calculated total energy (eV)	-6126.7656634	-6128.1803049
Recently Calculated energy differences (eV)	0	~ 1 [1]
Calculated energy differences	0	1.41464144
Calculated magnetic moment (Bohr mag/cell)	-	3.84
Experimental magnetic moment (Bohr mag/cell)	-	3.92 [6, 11]

Table 4.1 The comparison between recently calculated, experimentally calculated and computationally calculated for the ideal cubic structure of $BiMnO_3$

From the above table we see that the stable phase is the ferromagnetic phase, which is lower in energy. The energy difference between the two is 1.4 eV in which the ferromagnetic is more stable than the paramagnetic but the results have some difference from the computationally done paper because, the recent work [1] was done by using the experimental lattice parameter 3.95 Å.

In the above sections we presented the results which have been done by using the ideal cubic structure, which agreed to the paper [1]. A typical output file for a simple cubic ferromagnetic structure is given in appendix A.

4.3 Results for energy minimization by simple relaxation

Before we go to the vc-relax we did the simple relaxation (structure distortions) so as to minimize the energy. The minimum energy is one in which cubic symmetry is broken, and Mn atom and the oxygen cages are displaced from the initial configuration. When such process happened, a microscopic electric dipole is created in each unit cell, and this is reinforced by the interactions with the dipoles in all other unit cells. This is a material what we call it ferroelectric that displays a macroscopic non-zero polarization. This is exactly happened in the Figure 4.6 which presented as follows

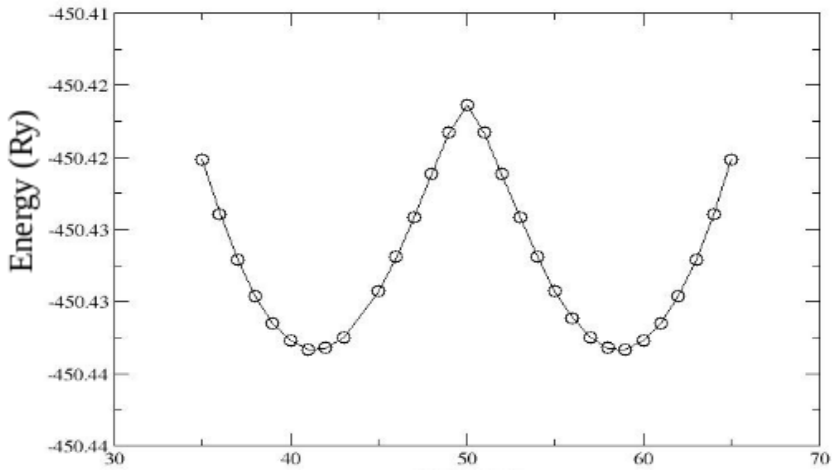

Displacement of Mn atom (a.u)

Figure 4.6 Displacing Mn, allowing the Oxygen cage to relax each time

When the Mn atoms are displaced from their original position both to the right and left by starting from a high symmetry configuration, which is maximum in energy, letting the O cage free to relax, the PWscf stops ionic relaxation fairly quickly because the forces on the O are very small. Only for the Mn displacement of 0.09 a.u., all of the sudden the forces on the O are large enough that the O cage starts moving off center, and falls into the lower potential energy surface. We find that there is an energy minimum at the displacement of 0.666 a.u. The energy difference between the two states $\Delta E = 0.2389$ eV, but if we displace the Mn by keeping the O cage in the symmetric cubic position it is just a parabola (Figure 4.7).

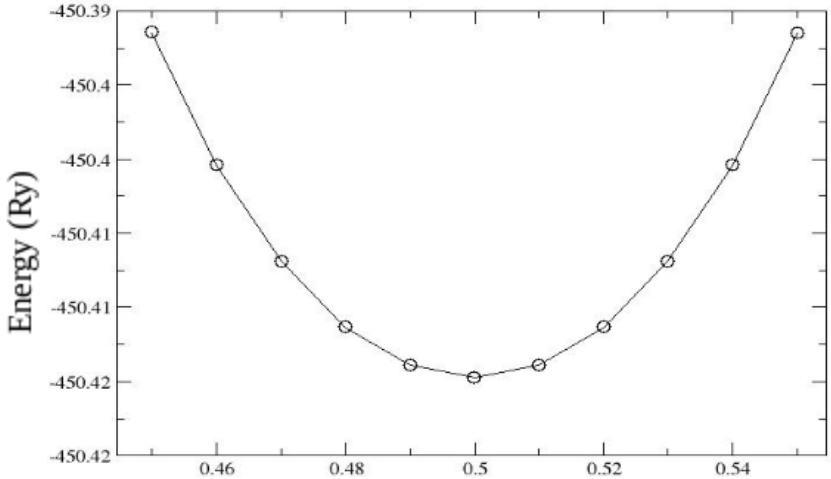

Figure 4.7 Displacing Mn, fixing all other atoms (Bi and O)

4.4 The results of simple cubic ferromagnetic after vc-relax

After simple relaxation the energy minimization processes continues and we did the vc-relax for our system. In simple relaxation we displace the atoms and find the minimum energy where it could be but in the case of vc-relax we displace the atoms and also change the volume of the system, and let the system to find its ground system. The results are displayed in Fig 4.8 and 4.9.

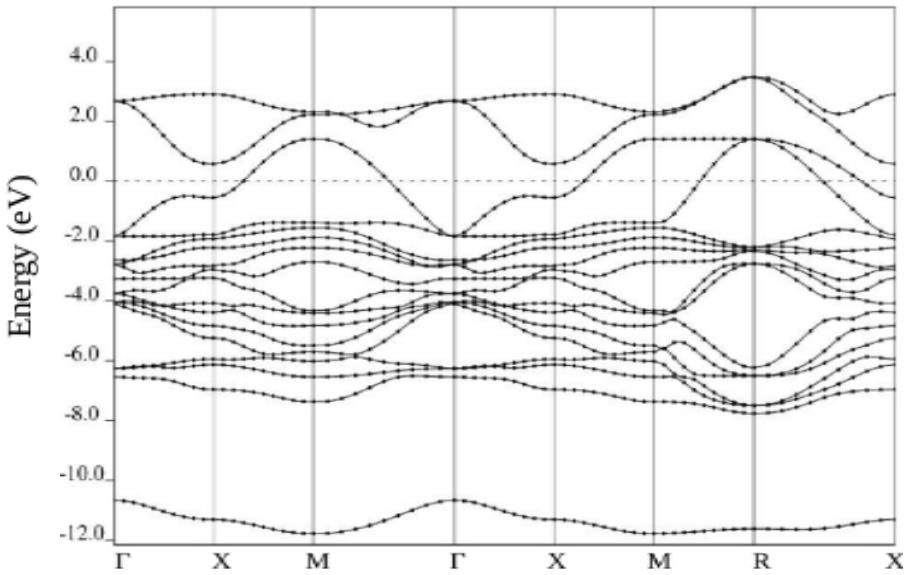

Figure 4.8.Spin up band structure for cubic ferromagnetic $BiMnO_3$ along the high symmetry axes of the Brillouin zone.

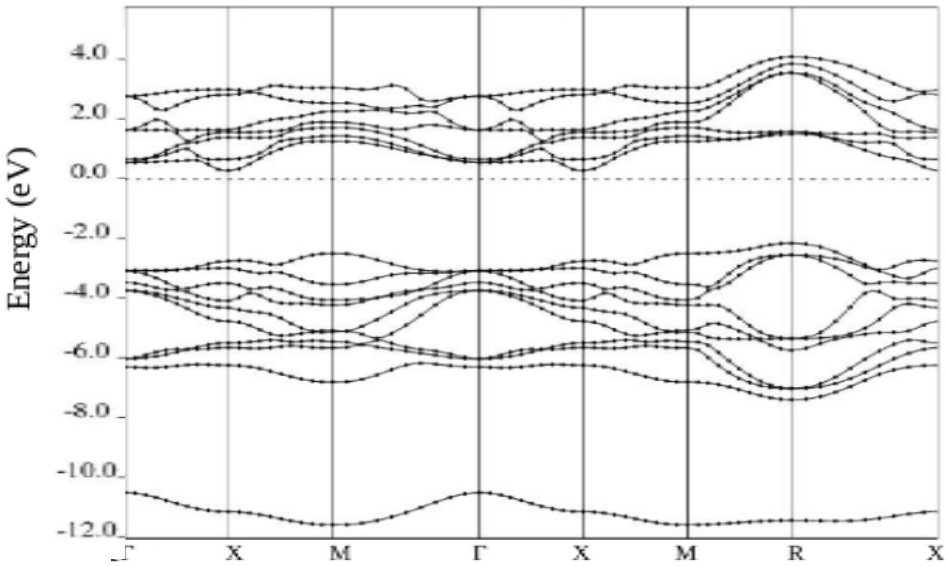

Figure 4.9.Spin down band structure for cubic ferromagnetic $BiMnO_3$ along the high symmetry axes of the Brillouin zone.

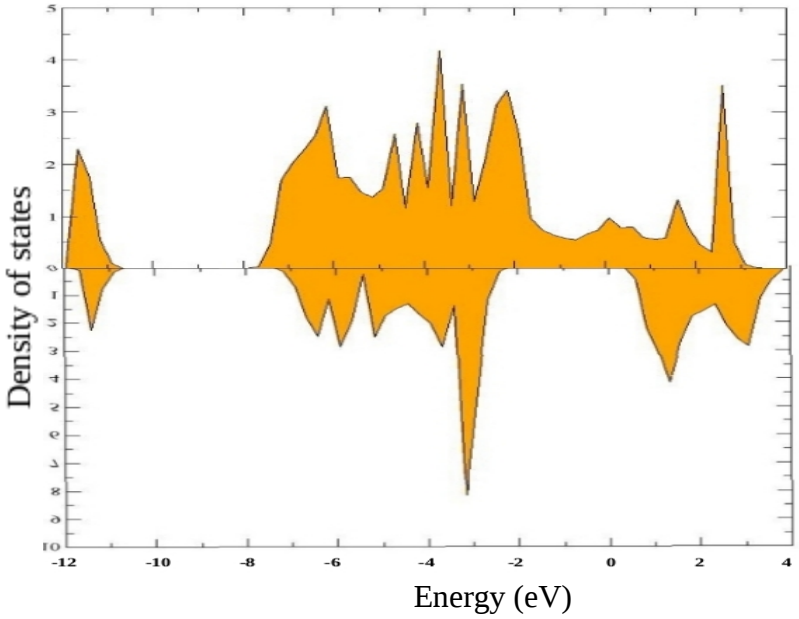

Figure 4.10. Spin up (top) and Spin down (bottom) density of state of the simple cubic ferromagnetic structure of $BiMnO_3$ along the high symmetry axes of the Brillouin zone.

In the above figures those states crossing the Fermi level are dominated by Mn 3d states hybridizing with O 2p states and the failure in having insulating property must be attributed to the shortcoming of GGA: often fails in describing the insulating property for strongly correlated electron systems. One way to cast the problem is to use GGA+U which are presented in the next section.

4.5 The results for simple cubic ferromagnetic structure of $BiMnO_3$ with Hubbard U

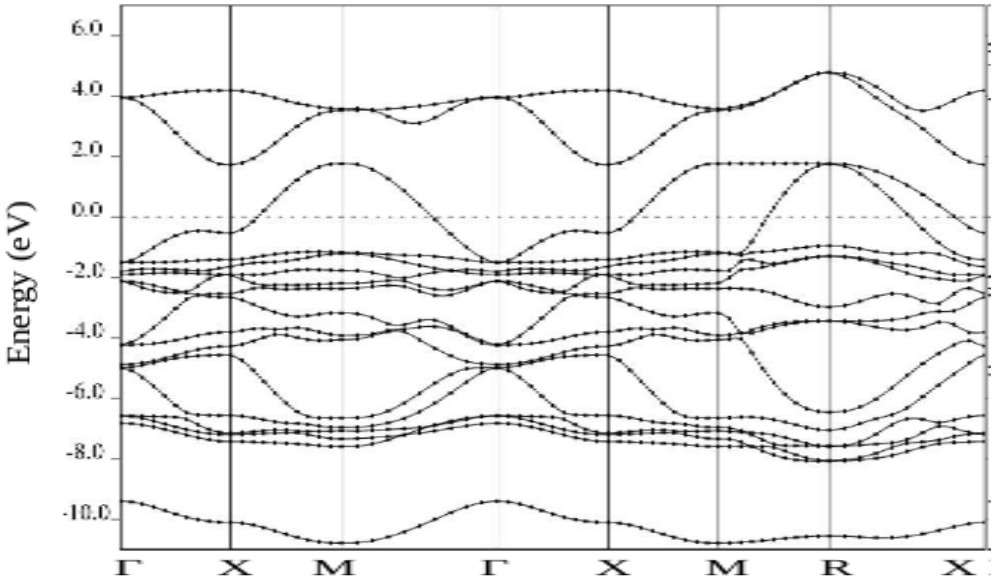

Figure 4.11.Spin up band structure of cubic ferromagnetic structure of $BiMnO_3$ with Hubbard U

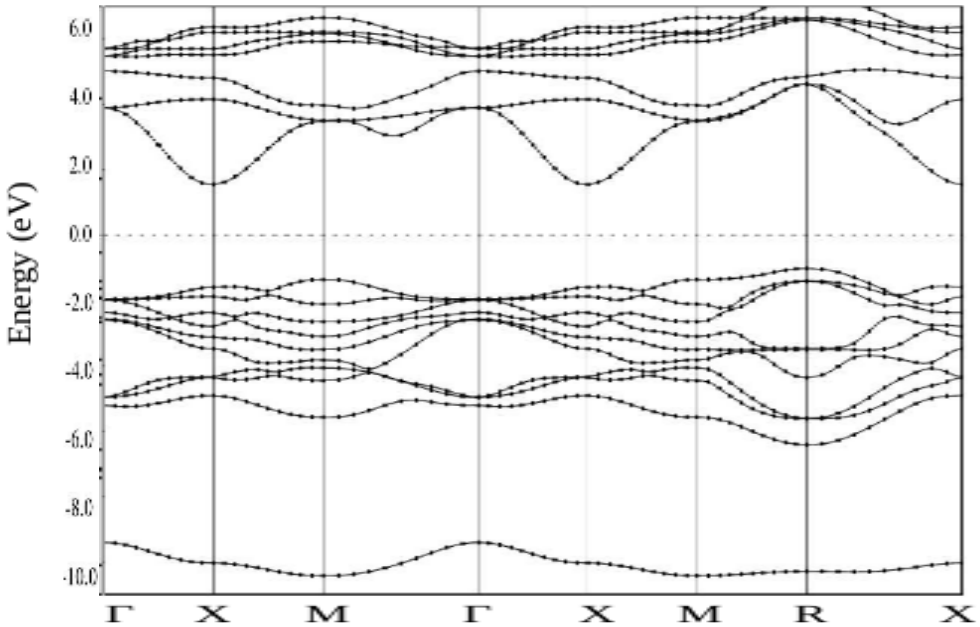

Figure 4.12 Spin down band structure of cubic ferromagnetic structure of $BiMnO_3$ with Hubbard U term

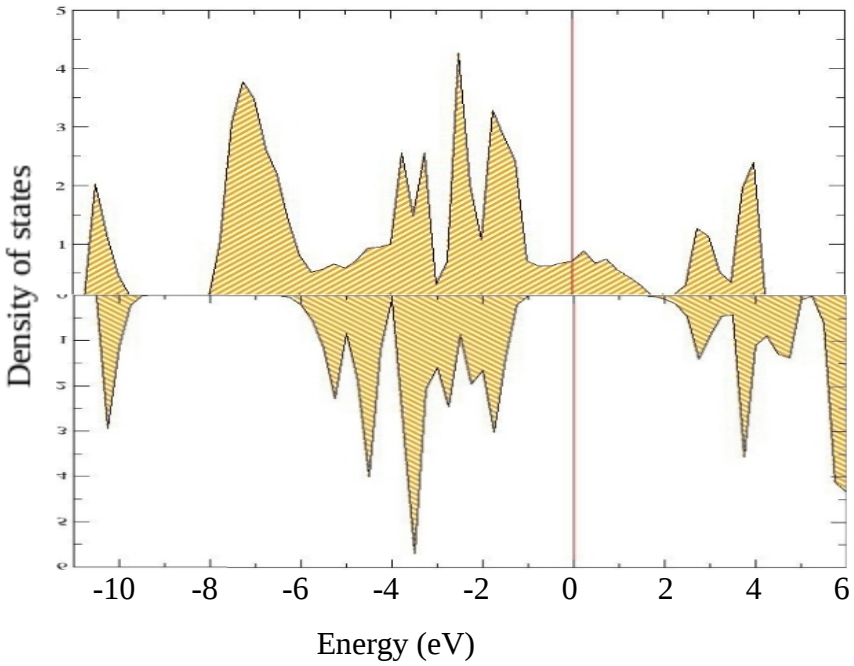

Figure 4.13.Spin up and Spin down density of state of cubic ferromagnetic structure of $BiMnO_3$ with Hubbard U term

When we switch on the Hubbard U term, the band gap further enhanced but unfortunately the band gap cannot be obtained for the majority spins state. Instead, a half metallic electronic structure is achieved with a gap in the minority spin.

In this study we use GGA+U method, where a Hartree-Fock type potential is alternatively adopted to specific states causing trouble, in the current case, Mn 3d states. In this method we use 8 eV for the parameter U.

As shown in Figure 4.11. The majority-spin 3d states are pushed down. We get a direct band gap of 2 eV at M and an indirect band gap of 0.3 eV between X and M. For the minority – spin 3d states in Figure 4.12 the band gap is further enhanced. The instability of the lattice can be confirmed from the calculation of phonon dispersion, which is presented in the next section.

4.6 The results of phonon dispersion simple cubic ferromagnetic structure $BiMnO_3$

The perovskite manganite have five atoms per unit cell, which results in 15 phonon branches, 3 acoustical and 12 optical. The results of phonon dispersion of $BiMnO_3$ are displayed in Fig 4.14 and 4.15

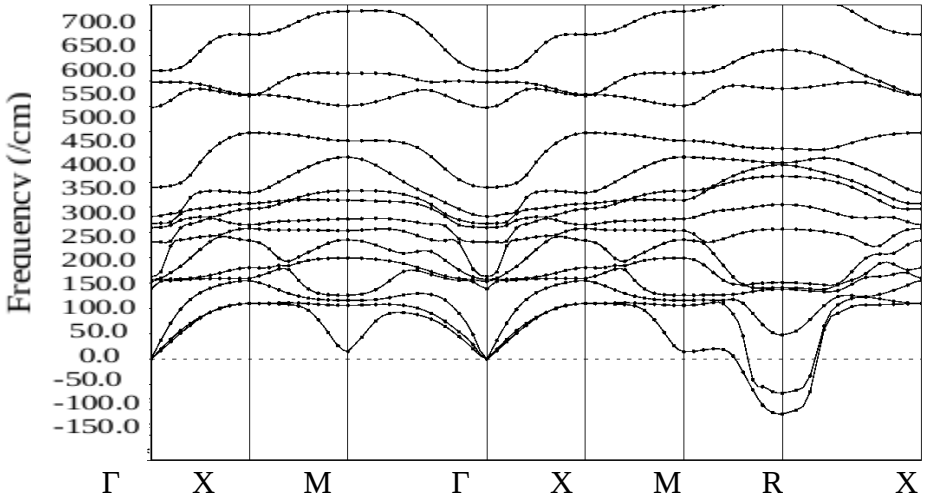

Figure 4.14 Phonon dispersion of the simple cubic ferromagnetic $BiMnO_3$

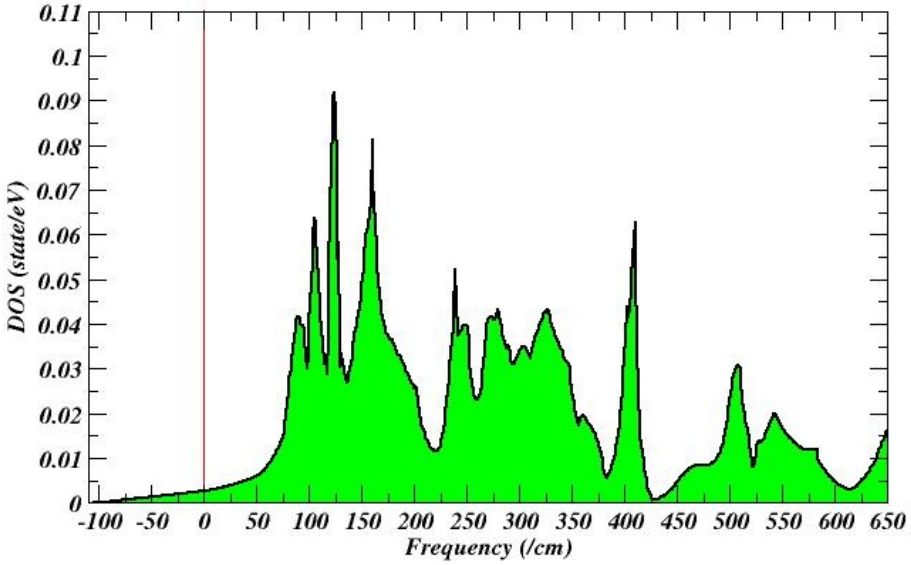

Figure 4.15 Phonon dispersion Density of state of the simple cubic ferromagnetic $BiMnO_3$

At the Γ point all phonons are three fold degenerate, there is one acoustical phonon frequency (which is zero), and four optical frequencies. The large Bi ions are moving in opposite to the oxygen cage, resulting in ferroelectric displacement. The Mn is moving in the same direction to oxygen ion. This observation is new and requires further investigations. A typical phonon output file for the first q at the gamma point is given in appendix B.

Chapter five

Conclusion and future outlook

5.1 Conclusion

From the first principles calculation using Quantum-ESPRESSO package, the electronic structure, magnetic properties and lattice instabilities of cubic $BiMnO_3$ are calculated using a generalized gradient approximation (GGA) within density functional theory. The results are first done without Habbard U and we get a well agreed result for both the experimentally done and computationally done papers from the first principle also. Adding a Hubbard U term further enhances the calculation. Even if a full band gap is not achieved for the majority carriers, it shows a better result. But the considerable band gap is achieved in the minority carriers which we call it a half-metallic system which considered desirable for devices of spin transistors, spintronics, etc. From the energy minimization we deduce that the material can undergo a ferroelectric phase, which can be used as a ferroelectric material in memory.

The phonon dispersion clearly shows that the cubic ferromagnetic $BiMnO_3$ have an imaginary frequency, which indicates that the $BiMnO_3$ is strongly unstable. Our results indicate that covalent bonding between the bismuth cations and Oxygen anions in $BiMnO_3$ introduces an additional orbital interaction which stabilize different magnetic and structural phases.

5.2 Future outlook

In this thesis research we did for a simple cubic ferromagnetic structure of $BiMnO_3$ from the first principle with DFT. The calculation is done with a general gradient approximation with a Hubbard U term correction. The insulating property is not achieved to the majority carriers, which enhances the science to seek once again to the GGA+U for strongly correlated systems of perovskites. It is also expected to take part on the monoclinic structure of the $BiMnO_3$, which limits us due to a computational cost.

Researchers who are working around spintronics devices, they can do experiment on ferromagnetic $BiMnO_3$ to achieve ferromagnetic configuration to be stabilized.

Appendix A

The output file for a simple cubic ferromagnetic structure of $BiMnO_3$

```
  the Fermi energy is    12.1635 ev
!    total energy              =  -450.44375209 Ry
     Harris-Foulkes estimate   =  -450.44375209 Ry
     estimated scf accuracy    <        4.9E-12 Ry
     The total energy is the sum of the following terms:
     one-electron contribution =  -205.96367732 Ry
     hartree contribution      =   129.96452277 Ry
     xc contribution           =   -60.86678652 Ry
     ewald contribution        =  -313.57533628 Ry
     smearing contrib. (-TS)   =    -0.00247475 Ry
     total magnetization       =     3.99 Bohr mag/cell
     absolute magnetization    =     4.15 Bohr mag/cell
     convergence has been achieved in  16 iterations
     Forces acting on atoms (Ry/au):
     atom   1 type  1   force =     0.00000945   -0.00001055    0.00000691
     atom   2 type  2   force =     0.00000969    0.00000481   -0.00001206
     atom   3 type  3   force =    -0.00000111    0.00000567    0.00000250
     atom   4 type  3   force =     0.00000152    0.00000178    0.00000553
     atom   5 type  3   force =    -0.00001955   -0.00000171   -0.00000289
     Total force =     0.000031     Total SCF correction =     0.00000000
     entering subroutine stress ...
          total   stress  (Ry/bohr**3)                   (kbar)     P=    0.00
   0.00000005   0.00000000   0.00000004          0.01      0.00      0.01
   0.00000000  -0.00000005   0.00000005          0.00     -0.01      0.01
   0.00000004   0.00000005   0.00000006          0.01      0.01      0.01
```

Appendix B

A typical output file for a phonon dispersion in a simple cubic FM $BiMnO_3$ for q1

omega(1) = 1.804318 [THz] = 60.185977 [cm-1]

(0.293578 0.000000 0.382737 0.000000 0.655047 0.000000)

(0.141175 0.000000 0.185307 0.000000 0.309183 0.000000)

(-0.073699 0.000000 0.152591 0.000000 0.111582 0.000000)

(0.115341 0.000000 -0.044444 0.000000 0.094440 0.000000)

(0.170497 0.000000 0.176780 0.000000 0.250381 0.000000)

omega(2) = 1.817247 [THz] = 60.617227 [cm-1]

(0.588546 0.000000 -0.538233 0.000000 0.051387 0.000000)

(0.288632 0.000000 -0.266295 0.000000 0.024482 0.000000)

(0.176440 0.000000 -0.225848 0.000000 -0.103070 0.000000)

(0.243293 0.000000 -0.189024 0.000000 0.120582 0.000000)

(0.053915 0.000000 -0.030364 0.000000 0.020093 0.000000)

omega(3) = 2.053251 [THz] = 68.489543 [cm-1]

(0.265973 0.000000 0.263904 0.000000 -0.281139 0.000000)

(0.268232 0.000000 0.267594 0.000000 -0.245182 0.000000)

(0.267407 0.000000 0.282556 0.000000 -0.209608 0.000000)

(0.282596 0.000000 0.267809 0.000000 -0.208837 0.000000)

(0.249974 0.000000 0.251099 0.000000 -0.246763 0.000000)

omega(4) = 3.881336 [THz] = 129.468285 [cm-1]

(0.053356 0.000000 -0.053506 0.000000 0.000005 0.000000)

(-0.267860 0.000000 0.267513 0.000000 0.000339 0.000000)

(-0.295970 0.000000 0.329339 0.000000 -0.113927 0.000000)

(-0.329343 0.000000 0.296421 0.000000 0.115523 0.000000)

(-0.465050 0.000000 0.464743 0.000000 0.000571 0.000000)

omega(5) = 4.159699 [THz] = 138.753547 [cm-1]

(-0.039621 0.000000 -0.039699 0.000000 -0.048196 0.000000)

(0.163627 0.000000 0.162705 0.000000 0.327123 0.000000)

(0.338188 0.000000 0.196687 0.000000 0.422565 0.000000)

(0.197252 0.000000 0.338493 0.000000 0.423007 0.000000)
(0.104819 0.000000 0.103881 0.000000 0.385302 0.000000)
omega(6) = 5.831228 [THz] = 194.510126 [cm-1]
(0.004455 0.000000 -0.004299 0.000000 -0.000043 0.000000)
(-0.014787 0.000000 0.014081 0.000000 -0.000197 0.000000)
(-0.420247 0.000000 0.012257 0.000000 -0.394179 0.000000)
(-0.012706 0.000000 0.420730 0.000000 0.394265 0.000000)
(0.408595 0.000000 -0.409682 0.000000 0.000091 0.000000)
omega(7) = 6.300930 [THz] = 210.177811 [cm-1]
(0.143295 0.000000 0.143679 0.000000 -0.149857 0.000000)
(-0.369927 0.000000 -0.370549 0.000000 0.407578 0.000000)
(-0.173815 0.000000 -0.305495 0.000000 0.190786 0.000000)
(-0.305149 0.000000 -0.175049 0.000000 0.189731 0.000000)
(-0.184083 0.000000 -0.183339 0.000000 0.329998 0.000000)
omega(8) = 8.305681 [THz] = 277.049548 [cm-1]
(0.036677 0.000000 -0.037476 0.000000 -0.001040 0.000000)
(-0.338802 0.000000 0.348085 0.000000 0.008028 0.000000)
(0.312966 0.000000 0.006799 0.000000 0.197702 0.000000)
(-0.007645 0.000000 -0.331271 0.000000 -0.216277 0.000000)
(0.481651 0.000000 -0.485380 0.000000 0.000274 0.000000)
omega(9) = 8.387938 [THz] = 279.793347 [cm-1]
(-0.022470 0.000000 -0.020988 0.000000 -0.041855 0.000000)
(0.206885 0.000000 0.192763 0.000000 0.370457 0.000000)
(-0.429190 0.000000 -0.000053 0.000000 -0.461635 0.000000)
(0.000160 0.000000 -0.414681 0.000000 -0.451867 0.000000)
(-0.065907 0.000000 -0.045806 0.000000 -0.014441 0.000000)
omega(10) = 10.779458 [THz] = 359.566390 [cm-1]
(0.020307 0.000000 0.020509 0.000000 -0.018390 0.000000)
(0.178687 0.000000 0.178127 0.000000 -0.177375 0.000000)
(-0.303522 0.000000 -0.203783 0.000000 0.346608 0.000000)
(-0.202263 0.000000 -0.302165 0.000000 0.346158 0.000000)

(-0.416598 0.000000 -0.415325 0.000000 0.227662 0.000000)

omega(11) = 11.321817 [THz] = 377.657678 [cm-1]

(-0.006696 0.000000 -0.006721 0.000000 -0.018866 0.000000)

(-0.003272 0.000000 -0.003080 0.000000 -0.051472 0.000000)

(-0.393901 0.000000 -0.025423 0.000000 0.236686 0.000000)

(-0.025309 0.000000 -0.393410 0.000000 0.237121 0.000000)

(0.535686 0.000000 0.534924 0.000000 0.017868 0.000000)

omega(12) = 11.478601 [THz] = 382.887457 [cm-1]

(-0.014657 0.000000 0.014679 0.000000 -0.000025 0.000000)

(-0.025742 0.000000 0.025917 0.000000 -0.000159 0.000000)

(0.427282 0.000000 0.014726 0.000000 -0.553785 0.000000)

(-0.014776 0.000000 -0.427573 0.000000 0.554315 0.000000)

(-0.096323 0.000000 0.095867 0.000000 0.000230 0.000000)

omega(13) = 14.693024 [THz] = 490.109796 [cm-1]

(-0.001376 0.000000 -0.002759 0.000000 -0.003874 0.000000)

(-0.044055 0.000000 -0.088315 0.000000 -0.124867 0.000000)

(-0.100892 0.000000 0.511932 0.000000 -0.152354 0.000000)

(0.253578 0.000000 -0.145005 0.000000 -0.174856 0.000000)

(-0.003496 0.000000 -0.067547 0.000000 0.747463 0.000000)

omega(14) = 14.715505 [THz] = 490.859681 [cm-1]

(0.003911 0.000000 -0.003053 0.000000 0.000745 0.000000)

(0.125199 0.000000 -0.098856 0.000000 0.024707 0.000000)

(0.134929 0.000000 0.578390 0.000000 0.089223 0.000000)

(-0.728279 0.000000 -0.087853 0.000000 -0.023005 0.000000)

(0.168005 0.000000 -0.155452 0.000000 -0.148952 0.000000)

omega(15) = 16.339449 [THz] = 545.028980 [cm-1]

(-0.003658 0.000000 -0.003692 0.000000 0.003859 0.000000)

(0.059409 0.000000 0.058849 0.000000 -0.058395 0.000000)

(0.195981 0.000000 -0.497234 0.000000 -0.205204 0.000000)

(-0.499985 0.000000 0.195642 0.000000 -0.205289 0.000000)

(0.194795 0.000000 0.194438 0.000000 0.505610 0.0000

References

[1] Nicola A.Hill and Karine Rabe, Phys. Rev B, **59** 8759, 1999.

[2] Alessio Fillippetti and Nicola A.Hill, Phys. Rev B, **65** 195120, 2002.

[3] M.Ghitta, M.Fornari, D.J.Singh and S.V Halivov, Phys. Rev B, **72** 054114, 2005.

[4] T. Atou, Y.Yamaguchi, K.Ohoyama and H. Chiba, A.Moreira dos Santos and A.K. Cheetman, Phys. Rev B, **66** 064425, 2002.

[5] IV Solovey and ZV Pehelkina, New J. Phys., **10** 073021, 2008.

[6] Katsuaki Kodama, Satoshi Iikubo,Shin-ichi Shamoto, Alexi A.BELIK, and Eiji TAKAYAMA-MUROMACHI, J. Phys. Soc. Jpn., **76** 12, 2007.

[7] Kimura T, Kawamoto S.yamada I, Azuma M, Takama M and Tokura Y, Phys. Rev B, **67** 180401(R), 2003.

[8] Chiba H, Atou T and SyoneY , J. Solid State Chem., **132** 139, 1997.

[9] T.Atou, H.Chiba, K.Ohoyama, Y.Yamaguchi, and Y.Syono, J. Solid State Chem., **145** 639, 1999.

[10] Alexi A. Belik, Satashi Likubo, Tadahiro Yokosawa, Katsuaki Kodama, Naoki Igawa, Shinichi Shamoto, Masaki Azuma, Mikio Takano, Koji Kimito , Yoshio Matsui, and Eiji Takayama Muromachi, J. Am. Chem. Soc., **129** 971, 2007.

[11] Pio Baeting, Ram Seshadri Nicola Spaldin, J. Am. Chem. Soc., **129** 9854, 2007.

[12] R.D King-Smith and David Vanderbilt, Phys. Rev B, **49** 5828, 1994.

[13] David Vanderbilt, First principles based modeling of ferroelectrics, **2** 701, 1997.

[14] David Jiles, Introduction to the Electronic properties of Materials, Nelson Thormes, 2001.

[15] http://www.PWscf.org, May 10.

[16] Hand Zeina, First principles and model calculations of manganites, Univesistat Stuttgart, 2008.

[17] Richard M.Martin, Electronic Structure, Basic Theory and practical methods, Cambridge, U.K., 2005.

[18] Efthimios Kaxiras, Atomic and Electronic Structure of Solids, Cambridge university press, New York., 2003.

[19] Paolo Giannozi, Metodi Numerica in Struttura Electronica, Anno Accadamico., 2007/2008.

[20] Anderson PW, Phys. Rev, **124** 41, 1961.

[21] Vladmir I Anisimov, F Aryasetiawan and A I Lichtenstein, J. Phys. Condens. Matter, **9**

767-808, 1997.

[22] Fujimor A and Minami F, Phys. Rev B, **30** 957, 1984.

[23] Van Elp J, Potze R.H, Eskes H,Berger R and Sawatzky GA, Phys. Rev B, **42** 5459, 1991.

[24] Phillips J.C., Phys. Rev, **112** 685, 1958.

[25] YIN M.T., and M.L Cohen, Phys. Rev B, **25** 7403, 1982a.

[26] YIN M.T., and M.L Cohen, Phys. Rev B, **25** 7403, 1982b.

[27] Cohen M.L., and V.Heine, Solid State Physics, **24** 37, 1970.

[28] Joannopoulos J.D., T.Starkloff, and M.A Kastner, Phys. Rev Lett., **38** 660, 1958.

[29] Starkloff T., J.D. Joannopoulos, Phys. Rev B, **16** 5212, 1977.

[30] Shirly, E.L.,D.C., Allah R.M. Martin, and J.D.Joannopoulous, Phys. Rev B, **40** 3652, 1989.

[31] M.C Payne, M.P Teter and D.C Allan, T.A Arias and J.D Joannopoulos, Mod. Phys.Rev., **64** 4, 1992.

[32] Stefano Baroni,Stefano de Gironcoli, Andrea Dal Corso and Paolo Giazzoni, Mod. Phys. Rev., **73** 2, 2001.

[33] G..P Srivatava, The physics of phonons, IOP publishing Ltd., 1990.

[34] Charles Kittle, Introduction to Solid State Physics, Printed in USA., 1986.

DECLARATION

This thesis is my original work and has not been presented for a degree in any other university

Name MESFIN ATLAW

Signature _____

This thesis has been submitted for examination with my approval as university advisor

_____

Dr. S.K. GHOSHAL

_____

Date